Double skin façades integrating photovoltaics and active shadings: a case study for different climates

A. K. Athienitis[a], A. Buonomano[b*], Z. Ioannidis[a], K. Kapsis[a], T. Stathopoulos[a]

[a]Centre for Zero Energy Building Studies, Department of Building, Civil and Environmental Engineering, Concordia University, 1455 de Maisonneuve Blvd. W., Montreal, H3G 1M8 QC, Canada
[b]Department of Industrial Engineering, University of Naples Federico II, P.le Tecchio, 80, 80125 Naples, Italy

Abstract: In this paper the energy potential of an innovative Double Skin Façade integrating Photovoltaics (DSF-P) for different weather conditions is investigated. The proposed system consists of semi-transparent and opaque PV modules integrated in the exterior skin of the façade and active shading devices implemented within the cavity. The innovative single or multióstory proposed DSF can co-generate solar electricity and thermal energy (for space heating or other building applications). In order to effectively cool down the photovoltaics and increase their electrical efficiency, the buoyancy-driven air flow within the cavity may be assisted by a fan (natural / hybrid ventilation). Active roller blinds are taken into account to regulate heating and cooling loads while controlling the daylight in the corresponding adjacent indoor spaces. With the aim to simulate the system performance, the temperature distribution and the airflow in the DSF, a mathematical model was developed. It is also capable to predict the energy flow, as well as the active and passive effects of the DSF-P on the energy consumption of the adjacent perimeter zones. The simulation model is based on a detailed transient finite difference thermal network, including accurate algorithms for the calculation of the heat transfer phenomena taking place within the DSF-P. The model, also allows performing parametric and sensitivity analyses, useful for pre-feasibility studies at the design phase of new buildings or for retrofit projects implementing the proposed DSF-P. In this paper, in order to determine the values of critical design and operating parameters that minimize the overall energy consumptions, a parametric analysis is carried out. Thus, a case study related to a high-rise office building located in diverse climate zones is presented. Simulation results show the effects due to some crucial DSF-P design and operation parameters on the energy demand of the adjacent zones, and the effectiveness of the proposed system to reach the goal of net zero energy building.

Keywords
Double Skin Façade with Photovoltaics, semi-transparent PV, energy performance analysis

1. Introduction

Buildings play a crucial role toward the reduction of energy consumptions and the achievement of climate goals, which can be achieved by the development and deployment of renewable technologies. Among the available technologies, solar based ones are considered as the most promising since they can be easily architectonically integrated within building façades, roofs, windows, etc. (COST Action TU1205 2015). Among novel facade design concepts, Double Skin Facades (DSF) have become an important architectural element, being capable to minimize the building energy demands while providing comfortable indoor climate, daylighting, sound and wind protection, aesthetic and structural advantages (Agathokleous and Kalogirou 2016). Recently, the use DSF, especially in combination with integrated PV panels (DSF-P), serving as building envelope material and power generator, is more significant than before (Agathokleous and Kalogirou 2016). In addition, by exploiting solar radiation, DSF-P may satisfy all the building energy needs, leading to the design and research of net-zero energy buildings (NZEB) (Athienitis and O'Brien 2015)

DSF-P consist of an external and an internal skin (i.e. the insulated façade of a newly built or

renovated building) separated by a cavity gap with air flowing in between. Opaque and semi-transparent PVs can be integrated within the exterior skin, giving the opportunity to design active and energy positive façades (generating electricity through PV, controlling solar heat gains and recovering heat for building energy uses) (Ghaffarianhoseini et al. 2016). The air cavity, that can act as a buffer zone, can be naturally or hybrid ventilated as well as equipped with fixed or movable shading devices, which have significant potential for daylight control and energy savings (Shameri et al., 2011).

DSF have been widely investigated and reviewed, with a particular focus on air flow and heat transfer aspects (De Gracia et al. 2013; Barbosa and Ip 2014), energy and comfort potentials (Shameri et al. 2011), numerical methods (De Gracia et al. 2013) and experimental approaches (Agathokleous and Kalogirou 2016). Despite of all research carried out on DSF, the available literature underlines a lack of studies for the investigation of the DSF advantages and its use for novel design configurations (Agathokleous and Kalogirou 2016). Specifically, very few studies have been carried out on the assessment of the daylighting and energy potential of DSF, especially when integrated with semi-transparent photovoltaics. Further research is also required to investigate the whole DSF-P system including its adjacent zones (Barbosa and Ip 2014; COST Action TU1205 2015). In this regard, there is still a lack of whole building simulation tools capable to model advanced DSF and DSF-P configurations, providing modelling flexibility with respect to the development of suitable DSF operation strategies (e.g. natural and hybrid ventilation, shadings control, heat recovery).

In this framework, in order to cover the lacks of knowledge regarding this research topic, the present work analyses the energy and economic potentials of a novel configuration of DSF-P particularly suitable for multi-story buildings. To this aim, authors developed a numerical model for the assessment of the energy performance of a DSF-P integrated with opaque or semi-transparent photovoltaics and equipped with movable shading devices installed inside the cavity. A case study analysis related to a high-rise office building located in different climate zones is carried out to assess the active and passive effects of such novel DSF-P system on the building energy consumptions, also toward the NZEB goal.

2. <u>Simulation Model</u>

This section includes a brief description of the mathematical model developed for the assessment of the energy performance of a multi-story DSF-P, integrating semi-transparent and opaque PVs, as well as movable roller shadings (Ioannidis Z. et al. 2016; Ioannidis Z. et al. 2016). The model, implemented in MatLab, allows calculating the active and passive energy performance of a novel DSF-P systems on the heating and cooling consumptions of the adjacent indoor air spaces. The numerical model can be used for pre-feasibility studies, in the early design stages of new or retrofit buildings to be integrated with DSF-P technology.

The modelled façade is depicted in Fig. 1a, showing a single thermal zone of a multi-story building (subdivided in Z different perimeter thermal zones, same as the number of the floors) implementing the DSF-P. The proposed DSF-P consists of a semi-transparent PV section, a so-called vision section (i.e. glazing), and an opaque PV section. The separation wall between the cavity and the indoor air consists of two opaque elements (i.e. spandrels located at the top and bottom of the wall) and a glazing area at the middle of the wall. The whole façade and the wall of a multi-story building can be designed as multiple strips made of semi-transparent, transparent, and opaque elements. Roller /blinds are located in the middle of the cavity in order to control the daylighting levels within the indoor space Fig. 1a. Air flows on both sides of the two cavity channels coupled via such blinds. The mathematical model of the DSF-P is based on the finite volume approach. A set of explicit equations is obtained for each node of the considered thermal Resistance Capacitance (*RC*) network, including conductive, radiative and convective heat transfers occurring within and through the modelled DSF-P system.
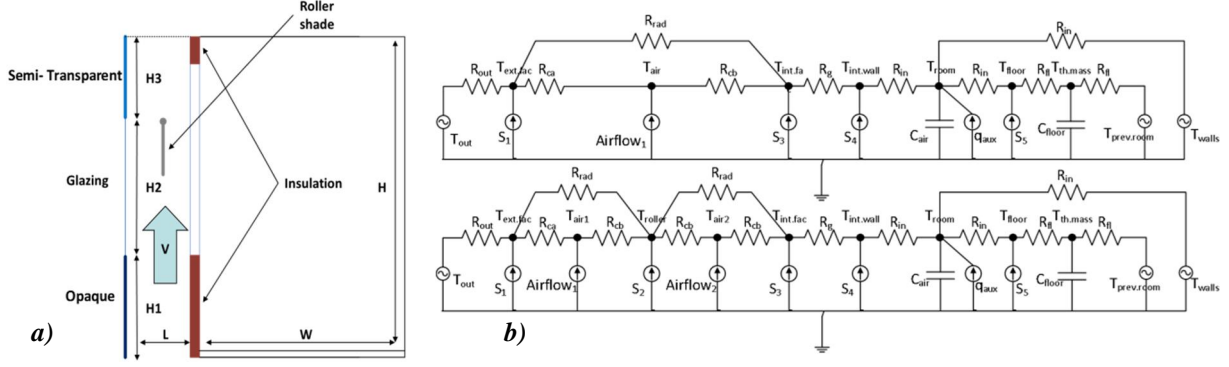
Fig. 1. Sketch of the modelled DSF-P (a) and RC thermal network (b)

A sketch of the *RC* thermal network is given in Fig. 1b. Each element of the multi-story DSF-P (i.e. the façade, the two air channels, and the wall) is subdivided, along the vertical direction, in N equal control volumes, whose temperatures are calculated through the energy balance method.

In each time step t, for each z-th perimeter zone and for each n-th section/node of the façade, the corresponding energy balance equation is calculated as:

$$\sum_{i=n-1}^{n+1} \frac{T_{f,i} - T_{f,n}}{R_{f,i}} + \frac{T_{out} - T_{f,n}}{R_{ext,n}} + \frac{T_{air,n} - T_{f,n}}{R_{ch,n}} + \dot{Q}_{f,n} + \dot{Q}_{rad,n} = 0 \qquad (1)$$

where T_f, T_{out} and T_{air} are the temperatures of the façade section, the ambient air and the cavity air; $R_{f,i}$ is the conductive resistance of each half sub-section of the façade, $R_{ext,n}$ is the external convective resistance and $R_{ch,n}$ is the convective resistance calculated within the channels/cavity. $\dot{Q}_{rad}$ accounts for the net radiation exchange, (sum of the incoming radiation directly absorbed by the surface and the radiative heat transfer between facade and sky); $\dot{Q}_f$ is the long-wave radiation exchange on the internal DSF surfaces. The radiative heat transfer problem within the channel takes into account view factors and radiosities of all the sections constituting the DSF cavities (i.e. between skins and roller shades) (Ioannidis Z. et al. 2016).

The buoyancy-driven air flowing inside the cavity is assumed to be quasi steady. According to previous studies, the change of energy of each n-th control volume is assumed equal to the energy transferred to the air by convection, calculated by (Charron and Athienitis 2006):

$$T_{air,n} = \exp\left(-\frac{R_{ch,n}^{-1} + R_{ext,n}^{-1}}{\dot{m}_{air} \cdot c_{p,air}} \right) \cdot T_{air,n-1} + \left[1 - \exp\left(-\frac{R_{ch,n}^{-1} + R_{ext,n}^{-1}}{\dot{m}_{air} \cdot c_{p,air}} \right) \right] \times \left(\frac{R_{ch,n}^{-1} \cdot T_{f,n} + R_{ext,n}^{-1} \cdot T_{wo,n}}{R_{ch,n}^{-1} + R_{ext,n}^{-1}} \right) \qquad (2)$$

where $\dot{m}_{air}$ and $c_{p,air}$ are the mass flow rate and the specific heat capacity of the flowing air.

The interior skin of the double skin façade is modelled through an exterior node, facing the cavity, and an interior one, facing the indoor space Fig. 1b. For each node of the interior skin, for each n-th control volume, the corresponding energy balance equations are calculated as:

$$\frac{T_{air,n} - T_{wo,n}}{R_{ch,n}} + \frac{T_{wi,n} - T_{wo,n}}{R_{wl,n}} + \dot{Q}_{wo,n} + \dot{Q}_{rad,n} = 0 \qquad \text{and} \qquad \frac{T_{wo,n} - T_{wi,n}}{R_{wl,n}} + \frac{T_{in,k} - T_{wi,n}}{R_{int,n}} + \dot{Q}_{wi,n} = 0 \qquad (3)$$

where $T_{wo,n}$ and $T_{wi,n}$ are the temperatures of the exterior and interior wall sections, T_{in} is the indoor air temperature of the z-th building space; R_{wl} is the conductive resistance of the wall and $R_{int,n}$ is the internal convective resistance. $\dot{Q}_{wo,n}$ and $\dot{Q}_{wi,n}$ are the effective solar radiation incident on the external and internal surfaces of the wall, including the diffuse solar radiation and the net (transmitted and/or absorbed) beam solar radiation, calculated by considering cast shadows due to façade surfaces and roller blinds (Ioannidis Z. et al. 2016).

The gross electrical power production, P_{el}, is obtained by assuming uniform solar radiation, $I_{f,n}$, on clean exterior PVs (operating at maximum power point condition), and the PV

efficiency, η_{pv}, as linearly decreasing with the operating temperature (Liao et al. 2007):

$$P_{el} = \eta_{PV} \cdot I_{f,n} \cdot A_n \tag{4}$$

The transient effects induced by the thermal mass is considered by means of the floor thermal mass, lumped in several capacitive nodes. Note that interior walls are considered as adiabatic and their thermal masses are disregarded. For each z-th zone, the differential equation describing the energy rate of change of each floor temperature node is calculated as:

$$T_{fl,z}^{t} = T_{fl,z}^{t-1} + \frac{\Delta t}{C_{fl,z}} \cdot \left(\dot{Q}_{fl,z} + \sum_{k=1}^{N} \frac{T_{wi,k} - T_{fl,z}^{t-1}}{R_{rad,k}} + \frac{T_{in,z} - T_{fl,z}^{t-1}}{R_{fl,int}} \right) \tag{5}$$

being T_{fl} and C_{fl} the temperature and the thermal capacitance of each floor capacitive node; R_{rad} is the radiative thermal resistance between the internal DSF wall surfaces and the floor surface, $R_{fl,int}$ is the combined convective and radiative thermal resistance between the indoor air and the floor; $\dot{Q}_{fl,z}$ is the solar heat source at the node.

For each z-th indoor space adjacent to the DSF-P, the indoor air is assumed as uniform and perfectly mixed, resulting in a single lumped indoor air temperature node. The energy rate of change linked to the indoor air mass is calculated as:

$$T_{in,z}^{t} = T_{in,z}^{t-1} + \frac{\Delta t}{C_{in,z}} \cdot \left(\dot{Q}_{in,z} + \sum_{k=1}^{N} \frac{T_{wi,k} - T_{in,z}^{t-1}}{\bar{R}_{int,k}} + \frac{T_{fl,z} - T_{in,z}^{t-1}}{R_{fl,int}} \right) \tag{6}$$

where C_{in} is the thermal capacitance of the indoor air, $\bar{R}_{int}$ is the combined interior convective and radiative thermal resistance, $\dot{Q}_{in,z}$ is the overall sensible heat gain networked to the indoor air node, including: i) convective sensible internal gains due to occupants, lights and equipment, ii) infiltration/ventilation thermal load, iii) sensible heat supplied to or removed from the building space to maintain the indoor air at the desired set point temperatures.

Finally, a simple radiosity daylight model is implemented in order to assess the illuminance levels on the work-plane and the energy consumed to artificially light the adjacent zones. In addition, thermal energy recovered by the air flowing through the DSF can be directly supplied, as free heating, to the air thermal zone or to the evaporator of a heat pump. For the assessment of the Coefficient of Performances (of air-to-air or air-to-water heat pumps/chillers), two methods can be followed: i) a manufacturers data look up approach, ii) recommended analytical equations. In both cases, COP and EER are calculated by means of its nominal values and as a function of the operating conditions and part-load ratio f_{PLR}.

3. Case study

The presented case study refers to a conventional high rise office building, with the Eastó West oriented longitudinal axis. The modelled DSF-P is installed on the South facing perimeter thermal zones. Fig. 2 shows a sample thermal zone of the Proposed building System (PS) configuration whose energy consumptions are compared to a Reference System (RS) configuration obtained by simulating the same building without DSF-P, but with the same shading strategy. The sample thermal zone dimensions are shown in Fig. 2, following the assumptions described in (Reinhart et al. 2013). The cavity width is set to be 0.5m and the minimum air velocity is set at 0.25m/s; if natural convection allows higher flow rates the fan is switched off. For the PS configuration, the DSF-P outlet air is exploited in winter to supply the evaporator of the adopted air-to-air heat pump for space heating (also serving the RS configuration). A roller shading is placed at the middle of the cavity (0.25m from both ends) and the transmittance of the STPV is set equal to 30%. The South interior skin façade consists of: i) a window (4-16-4 air filled double-glazed low-e system) with U-value = 1.28W/m²K; ii) an insulated wall with U-value = 0.24W/m²K or 0.48W/m²K, iii) floor/ceiling with U-value = 1.10W/m²K. The direct solar radiation transferred through the windows to the interior zone is assumed to be absorbed by the floor (absorption factor = 0.4). For such zone, a ventilation

rate of about 1.6Vol/h and a crowding index of 0.12 person/m^2 are taken into account. Interior thermal gains include people (90W/p) and equipment (5W/m^2). Finally, artificial lighting energy use, depending on daylighting illuminance, is calculated in order to provide 300lux on office desk level. The DSF cavity, operated in hybrid ventilation mode, is closed when the ambient air temperature is lower than the heating set point T$_{sp,heat}$ + 3°C.
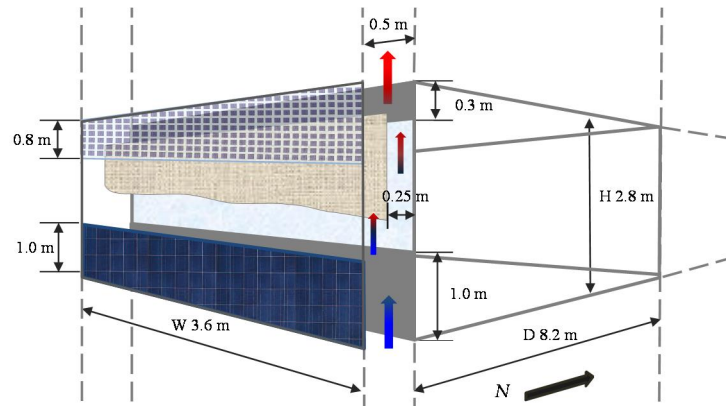
Fig. 2. Sketch of a sample perimeter thermal zone of the PS building configuration

Both the innovative (PS) and traditional (RS) buildings are simulated by taking into account a week-day schedule from 8.00 to 18:00 (week days only). The heating and cooling set points are 20°C and 26°C, maintained by an air-to-air electric heat pump/chiller. Two weather zones are considered: Naples (Italy, Mediterranean temperate climate) and Montreal (Canada, humid continental climate with very cold and snowy winter). They are simulated by taking into account Meteonorm weather data files. Simulations are carried out with one hour time step and starts on 0:00 of January 1st and ends at 24:00 of December 31st. The heating and cooling periods are shown in Table 1. Here, the heating and cooling degree days (HDD and CDD) and the incident solar radiation (ISR) indexes are also reported.

Table 1 - Climatic zones, climatic indexes and system scheduling.

Weather zone	HDD [Kd]	CDD [Kd]	ISR [kWh/m^{2}y]	Heating [hours]	Cooling [hours]
Montreal	4567	297	1350	15/Sep.-31/Mar.	1/Jun.-15/Sep.
Naples	1479	499	1470	15/Nov.-31/Mar.	1/Jun.-30/Sep.

4. Results and discussion

Fig. 3 shows the average monthly electricity production and maximum power output of a single thermal zone of the South-facing DSF-P, for both the investigated locations. In this figure it is possible to observe that the monthly energy output obtained during winter is much higher than that observed during summer. Specifically, the maximum monthly PV output is about 120kWh in March in Montreal and 115kWh in October in Naples; the minimum production is obtained in November in Montreal (47kWh) and in January in Naples (67kWh). Comparable annual results are calculated for the investigated weather zones: the total annual energy output of the DSF-P is about 1050kWh/y (162kWh/m^{2}y ó per PV area) in Montreal, and about 1083kWh/y in Naples (167kWh/m^{2}y ó per PV area). Note that, such results are due to average energy conversion efficiencies of the silicon crystalline semi-transparent and opaque PV modules of about 14% and 20%, respectively.

The DSF also enables flowing cold air to remove and/or recover a considerable amount of heat from PV panels improving their energy conversion efficiency; it also reduces solar heat gains and the space cooling load. Therefore, a proper design for the air ventilation cavity is crucial for the reduction of building energy use and the increase of the electricity production.
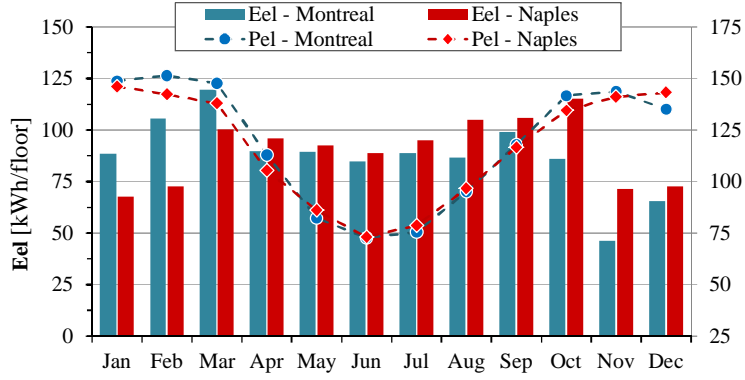
Fig. 3. Monthly average electricity production and maximum power output

Therefore, with the aim to optimize the cavity design and operation (minimizing the building overall energy demands), a sensitivity analysis was carried out by varying the air gap depth (**L**) and the minimum (i.e. of the fan) air velocity inside the channel (**v**). Their variation ranges are: 0.25 to 0.75 (with a step of 0.25m) and 0.2 to 1.0 (with a step of 0.2m/s), respectively. In Fig. 4a the overall annual electricity demand ($E_{el,TOT}$, due to the fan, heating, cooling, lighting and appliances), is reported as a function of **L** and **v**, for the weather zone of Naples. After an initial zone in which no variation is detected, $E_{el,TOT}$ considerably increases versus. both these parameters. By analysing the single contributions to $E_{el,TOT}$ (e.g. electricity for fan, heating, cooling, lighting and appliances, not reported for the sake of brevity), it was observed that by increasing the air gap depths (**L**): i) the air thermal resistance increases, reducing the heat transfer and the heating demand (particularly in case of occurring low solar radiation); ii) the lighting electricity demand increases due to a reduction of the daylighting illuminance inside the zone (higher daylighting reference points); iii) the energy demands for cooling decreases because of the reduction of solar gains.
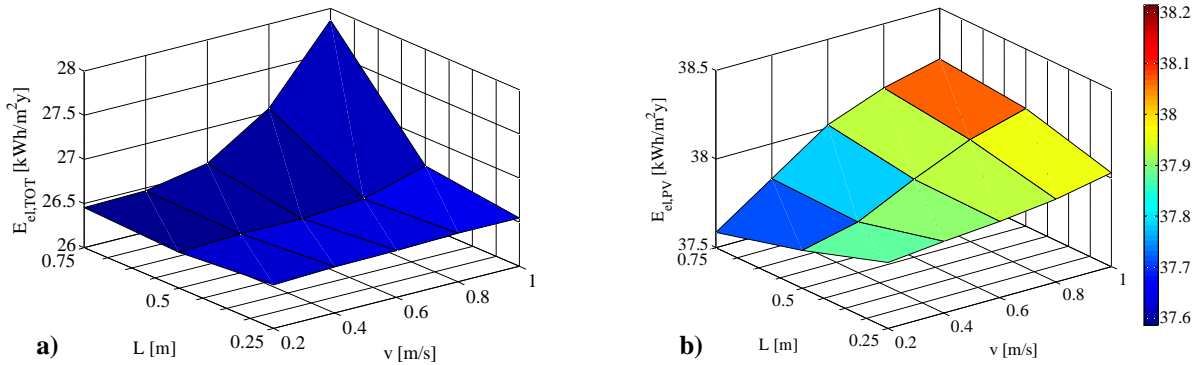
Fig. 4. Overall electricity consumptions $E_{el,TOT}$ (a) and PV production $E_{el,PV}$ (b) vs. L and v

Conversely, the variation of the PV electricity production versus. **L** and **v** is very small. Fig. 4b shows the variation trends of the annual electricity production ($E_{el,PV}$), occurring in Naples, as a function of **L** and **v**. $E_{el,PV}$ always increases with higher air velocities, whereas different trends are observed by varying **L**. Specifically, at low velocities a narrow gap boosts the air flow (stack effect), thus higher $E_{el,PV}$ are achieved, whereas for higher velocities, the wider the gap the higher $E_{el,PV}$. The integrated opaque and semi-transparent PV panels are capable to balance the annual overall electricity needs of the DSF-P adjacent thermal zones. In fact, the net electricity demand ($E_{el,PV} - E_{el,TOT}$) is positive for all the simulated cases, being $E_{el,PV}$ much higher than $E_{el,TOT}$. Very similar trends, for both $E_{el,PV}$ and $E_{el,TOT,}$ are observed in Montreal. Nevertheless, here due to the occurring cold winter, a much higher heating demand is

achieved. As a result, in both Naples and Montreal, the optimal values of **L** and **v**, resulted equal to 0.25 m and 0.2 m/s, respectively. It is also interesting to analyse the passive and active effects of the DSF on the heating needs. Fig. 5 shows the variation of the electricity demand for heating ($E_{el,Heat}$, heat pump compressor electricity) versus. **L** and **v**, calculated in Naples, when the DSF outlet air is: a) supplied to the evaporator of the heat pump; b) exhausted to the outside. Note that, the calculated $E_{el,Heat}$ of the reference system RS is equal to 74.5 kWh/y. From Fig. 5 it is evident the influence of passive and active effects due to the DSF on $E_{el,Heat}$. Specifically, Fig. 5a shows that $E_{el,Heat}$ is always lower than the RS demand, for any **L** and **v**: for low **L**, the higher **v** the higher $E_{el,Heat}$, whereas for high **L** the stack effect is reduced, producing lower $E_{el,Heat}$. In this regard, it is also worth noting that **v** is the minimum velocity of the air flow inside the channel, which is closed for ambient temperatures lower than $T_{sp,Heat} + 3°C$. Fig. 5b clearly shows that $E_{el,Heat}$ significantly decrease versus. the exhausted air case, thanks to the increase of the COP of the heat pump, obtained by supplying the DSF outlet air to its evaporator. The passive effect due to the reduction of the heat transfer through the DSF produces an average percentage reduction of the heating demand of the adjacent zone of about 3.2%, whereas both the effects, i.e. passive and active (due to the increase of the heat pump COP) lead to a reduction of about 16.7%. Note that although the presented results are related to the average building perimeter floor, simulations are carried out for a seven floor DSF-P / building system, which causes an average winter increase of the outlet temperature of about 11°C.
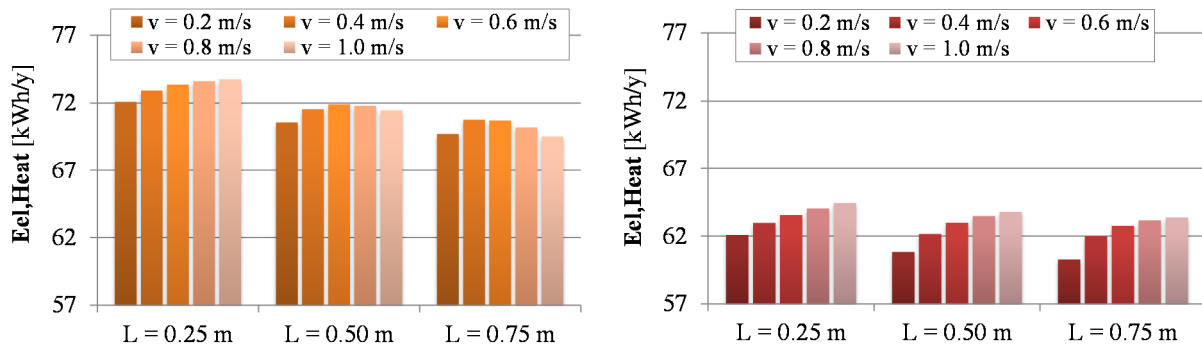
Fig. 5. Heating electricity demand $E_{el,Heat}$ vs. L and v. (a) with recovered heat, b) w/o recovered heat) - Naples

Such behaviour is less evident in Montreal due to the occurring very low winter temperatures. In fact, in Montreal, for the majority of the time, the DSF is closed (i.e. the ambient temperature is much lower than the DSF opening temperature, i.e. $T_{out} > T_{sp,Heat} + 3°C$). Therefore, there is a slight difference among the results obtained by supplying warmer air from the cavity to the evaporator of the heat pump or by exhausting it to the outside, whereas a reduction of $E_{el,Heat}$ of about 0.7% is observed (i.e. the RS demand is 620.5kWh/y).

Finally, in Table 2, the electricity demands due to heating, cooling, lighting, fans and equipment are reported, together with the produced PV panelsø electricity and the net electricity demands for both the RS (E_{RS}) and optimal PS (E_{PS}) configurations. The table also includes the percentage energy difference (E) for each energy use. By comparing E_{PS} with E_{RS}, it is worth noting that although the solar radiation is greatly exploited in both weather zones, i.e. Montreal and Naples (as shown in Fig. 3), in Naples, the investigated system allows reaching the NZEB goal (related to the adjacent thermal zones only), showing a surplus of electricity (about 357kWh/y, net demand). Differently, in Montreal due to the severe winter conditions (i.e. very high heating demands), the innovative solar façade is not able to completely balance the overall electricity demands of the adjacent zones; however, the overall electricity final demand, $E_{el,TOT}$, is reduced up to 79%.

Table 2 – Electrical performance of RS and PS configurations

	Naples			Montreal		
	E_{RS} [kWh/y]	E_{PS} [kWh/y]	E [%]	E_{RS} [kWh/y]	E_{PS} [kWh/y]	E [%]
Heating	*88.0*	*66.1*	*28.5*	*703.6*	*694.1*	*1.4*
Cooling	*158.8*	*137.7*	*13.3*	*95.0*	*90.0*	*5.2*
Lighting	*104.8*	*105.4*	*-0.5*	*111.3*	*111.6*	*-0.3*
Fan_{DSF} (×100)	*-*	*7.9*	*-*	*-*	*6.3*	*-*
Equipment	*420.8*	*420.8*	*0.0*	*420.8*	*420.8*	*0.0*
Total demand	774.8	760.9	1.8	1326.1	1316.1	0.8
PV production	*-*	*1118.1*	*-*	*-*	*1094.0*	*-*
Net demand	774.8	-357.2	146.1	1096.3	222.1	79.7

5. Conclusions

This paper presents a numerical model of a Double Skin Façade integrated with photovoltaics (DSF-P) able to assess the thermal and energy performance of the multi-story DSF-P system. With the aim to show the capability of the model, a case study is developed. It refers to a DSF-P installed on the South façade of a typical office building located in two different weather zones, Naples (Italy) and Montreal (Canada). Numerical results show that by means of the DSF-P system, the integrated opaque and semi-transparent PV panels can provide a high percentage of the electricity demands for energy uses. By introducing the preheated air of the DSF-P to the heat pump, an increase of the COP, particularly in the Mediterranean climate, is achieved. Such model may aid the design of net-zero energy buildings, by also performing parametric and sensitivity analyses useful for pre-feasibility studies at the design phase of new buildings or for retrofit projects implementing DSF-P.

Acknowledgments

References

Agathokleous, R. A. and S. A. Kalogirou (2016). "Double skin facades (DSF) and building integrated photovoltaics (BIPV): A review of configurations and heat transfer characteristics." Renewable Energy **89**: 743-756.

Athienitis, A. K. and W. O'Brien (2015). Modeling, Design, and Optimization of Net-Zero Energy Buildings.

Barbosa, S. and K. Ip (2014). "Perspectives of double skin façades for naturally ventilated buildings: A review." Renewable and Sustainable Energy Reviews **40**: 1019-1029.

Charron, R. and A. K. Athienitis (2006). "Optimization of the performance of double-façades with integrated photovoltaic panels and motorized blinds." Solar Energy **80**(5): 482-491.

COST Action TU1205 (2015). "Overview of BISTS state of the art, models and applications."

De Gracia, A., A. Castell, et al. (2013). "Numerical modelling of ventilated facades: A review." Renewable and Sustainable Energy Reviews **22**: 539-549.

Ghaffarianhoseini, A., A. Ghaffarianhoseini, et al. (2016). "Exploring the advantages and challenges of double-skin façades (DSFs)." Renewable and Sustainable Energy Reviews **60**: 1052-1065.

Ioannidis Z., Buonomano A., et al. (2016). A detailed dynamic model of multi-story double skin facades with integrated photovoltaic panels. eSim 2016 International Conference. IBPSA-Canada., Hamilton, ON, Canada.

Ioannidis Z., Buonomano A., et al. (2016). Double Skin Façades Integrating Photovoltaic Panels: A Comparative Analysis of the Thermal and Electrical Performance. Clima 2016 International Conference Aalborg, Denmark.

Liao, L., A. K. Athienitis, et al. (2007). "Numerical and Experimental Study of Heat Transfer in a BIPV-Thermal System." Journal of Solar Energy Engineering **129**(4): 423-430.

Reinhart, C. F., J. A. Jakubiec, et al. (2013). Definition of a reference office for standardized evaluations 2 of dynamic façade and lighting technologies. 13th Conference of International Building Performance Simulation Association, Chambéry, France.

Shameri, M. A., M. A. Alghoul, et al. (2011). "Perspectives of double skin façade systems in buildings and energy saving." Renewable and Sustainable Energy Reviews **15**(3): 1468-1475.